Magnetic structure of triangular lattice compound $Tb_2Ni_{0.90}Si_{2.94}$

Santanu Pakhira[a,b,*], A. V. Morozkin[c], Maxim Avdeev[d,e], Chandan Mazumdar[a]

[a] *Condensed Matter Physics Division, Saha Institute of Nuclear Physics, 1/AF, Bidhannagar, Kolkata 700064, India*

[b] *Ames Laboratory, Ames, Iowa 50011, USA*

[c] *Department of Chemistry, Moscow State University, Lenisnkie Gory, House 1, Building 3, Moscow, GSP-2, 119991, Russia*

[d] *Australian Nuclear Science and Technology Organisation (ANSTO), New Illawarra Rd, Lucas Heights, NSW 2234, Australia*

[e] *School of Chemistry, The University of Sydney, Sydney, New South Wales 2006, Australia*

Abstract

AlB_2-type ternary intermetallic compound $Tb_2Ni_{0.90}Si_{2.94}$ (space group $P6/mmm$, $hP3$, No. 191) was reported to exhibit spin freezing behaviour of the ferromagnetic clusters present in the system below $T_f = 9.9$ K, along with the presence of spatially limited antiferromagnetic phase. In this work, on the basis of variable temperature zero-field neutron diffraction measurements, we have shown that the antiferromagnetic phase transition occurs for the compound below $T_N \sim 13$ K. Neutron diffraction study indicates *ab*-plane non-collinear sine-modulated antiferromagnetic ordering of the system with wave vectors of $k_1 = [\pm 1/6, \pm 1/6, 0]$ and $k_2 = [\pm 1/3, \pm 1/3, 0]$ down to 1.7 K. The weak and diffuse nature of the magnetic Bragg peaks along with limited coherence length further confirm the short-range nature of the antiferromagnetic phase in this compound.

Keywords: Intermetallics, Rare-earths, Magnetic structure, Neutron diffraction

1. Introduction

During the last two decades, ternary intermetallic compounds of R_2TSi_3-type (R = rare-earth ions and T = transition metals) have generated significant interest due to their wide range of interesting physical properties, viz., frustrated magnetism, spin-glass behaviour, heavy-fermion behaviour, Kondo effect, mixed valence behaviour, large magnetocaloric effect, magnetoresistance, etc., besides conventional long-range magnetic ordering like ferromagnetism and antiferromagnetism[1, 2, 3, 4, 5, 6, 7, 8, 9, 10, 11, 12, 13, 14, 15, 16]. Recently, this class of materials have regenerated specific interest following the discovery of novel topologically protected skyrmionic spin texture in Gd_2PdSi_3 along with topological Nernst effect[17, 18, 19]. It is reported that magnetic frustration present in this compound plays a

*spakhira@ameslab.gov

Email address: santanupakhira20006@gmail.com (Santanu Pakhira)

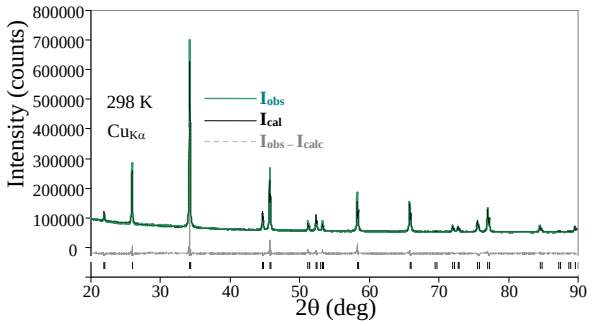

Figure 1: Room temperature (298 K) XRD pattern of as-cast $Tb_2Ni_{0.90}Si_{2.94}$ along with full-Rietveld refinement.

key role in stabilizing the skyrmion phase. Although depending on different T and X, these compounds crystallize in hexagonal crystal structure with space groups $P6/mmm$, $P\bar{6}2c$, and $P6_3/mmc$, most of the materials form in AlB_2-type crystal structure with space group $P6/mmm$. In this structure, the rare-earth ions are situated at the vertices of edge-sharing triangles forming a hexagonal layer. Two such hexagonal layers of R-ions are separated by a honeycomb layer of randomly distributed T and X ions[1]. Geometrical frustration arises in this structure in the presence of nearest-neighbour antiferromagnetic interaction among the R ions. Additionally, due to closeness of hexagonal lattice parameters a and c, magnetic frustration is also achieved when nearest-neighbour and next-nearest-neighbour exchange interactions are opposite of signs.

Earlier, we have reported that in the R_2NiSi_3 family of polycrystalline materials, Gd- and Er-based compositions form in single phase with full stoichiometry, while in case of other reported members considerable amount of secondary phase of $RNiSi_2$-type could also be detected and single phase nature could only be achieved by deliberately creating vacancies in the Ni and Si sites[7, 8, 10, 12, 20, 21, 22, 23, 24]. Recently, physical properties of one such member $Tb_2Ni_{0.90}Si_{2.94}$ are reported[23]. On the basis of dc magnetization, ac susceptibility and detailed studies on non-equilibrium dynamics it was reported that the compound undergoes spin-cluster glass behaviour below $T_f = 9.9$ K. However, zero-field neutron diffraction pattern measured at $T = 1.7$ K also suggest the presence of additional weak magnetic Bragg peaks which could not be indexed only with nuclear symmetry of the material, signifying the presence of additional antiferromagnetic interactions in this system [23]. In this work, we have studied the nature of magnetic structure of the as-cast $Tb_2Ni_{0.90}Si_{2.94}$ compound through temperature-dependent zero-field neutron diffraction measurements. The presence of non-collinear sine-modulated antiferromagnetic ordering is evidenced for the compound with limited coherence length below $T_N \simeq 13$ K.

2. Experimental details

Polycrystalline $Tb_2Ni_{0.90}Si_{2.94}$ compound was synthesized by standard arc-melting technique in argon atmosphere in an arc furnace. The ingots were melted six times with flipping

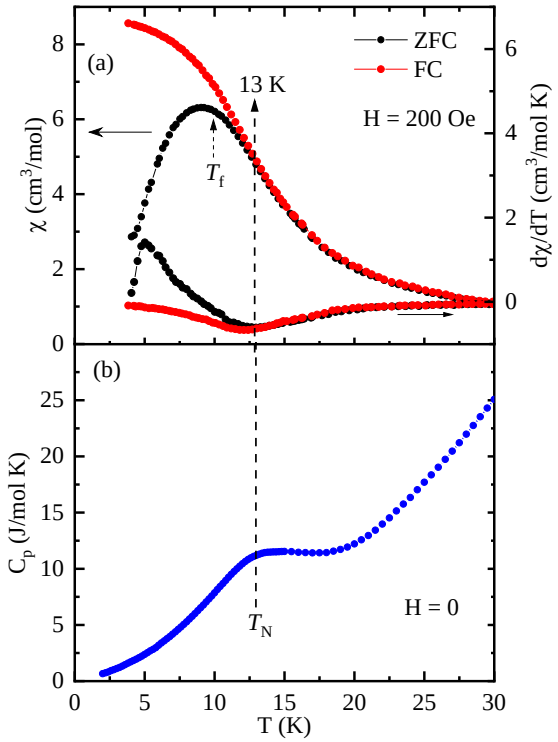

Figure 2: (a) Temperature dependence of dc magnetic susceptibility ($\chi = M/H$) at applied magnetic field $H = 200$ Oe under ZFC and FC conditions is shown in left panel. $d\chi/dT(T)$ is shown in the right panel. (b) T-dependence of $C_p(T)$ in the absence of magnetic field. T_N in the figures is marked based on the zero-field neutron diffraction results.

every time to ensure the volume homogeneity. Structural characterization was done by collecting the powder X-ray diffraction (XRD) pattern from a TTRAX-III difractometer (M/s Rigaku, Japan) using Cu-K_α radiation. The unit cell data were derived from the Rietveld analysis of the X-ray powder patterns, recorded at room temperature, using the Rietan program[25]. Variable temperature neutron powder diffraction data from 50 K to 1.7 K in zero applied magnetic field were collected using the Echidna diffractometer at the OPAL facility (Lucas Heights, Australia) with $\lambda_1 = 0.24395$ nm, $\lambda_2 = \lambda_1/2$, $I(\lambda_2)/I(\lambda_1) \sim 0.004$. A total of ~ 10 g sample were used for the neutron diffraction experiments. The structural and magnetic refinements were performed using the Rietveld refinement implemented in the FULLPROF software program[26]. The dc magnetic measurements were performed in a superconducting quantum interference device (SQUID) (M/s Quantum Design Inc., USA). The heat capacity measurement was done in a Physical Properties Measurement System (PPMS) (M/s Quantum Design Inc., USA) using relaxation technique.

3. Results and Discussions

Fig. 1 shows the room temperature powder X-ray diffraction (XRD) pattern of the compound along with full-Rietveld refinement. XRD analysis indicates that the compound forms

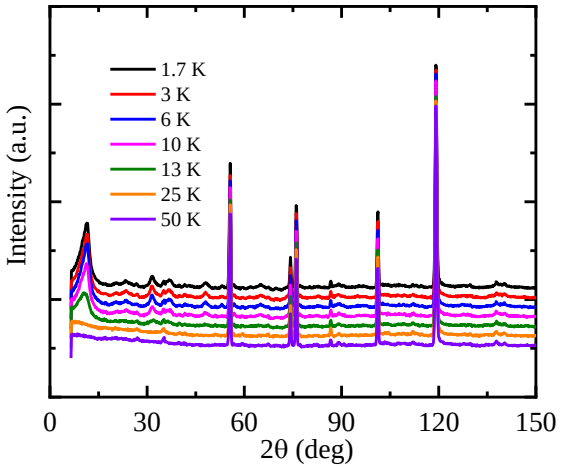

Figure 3: Neutron diffraction pattern of as-cast $Tb_2Ni_{0.90}Si_{2.94}$ measured at different temperatures. The spectra at different temperatures (except 50 K) were vertically shifted by constant amount for clarity. The features at the lowest 2θ in the diffraction patterns are due to instrumental artifacts.

in AlB_2-type structure (space group $P6/mmm$, $hP3$, No. 191) with lattice parameters $a = 0.39682(1)$ nm, $c = 0.40537(2)$ nm, $c/a = 1.02155$ and $V = 0.05525$ nm^3 ($R_f = 3.4\%$) similar to those reported earlier[23]. The substitution of Si for Ni leads to anisotropic distortion of unit cell of initial AlB_2-type $TbSi_{1.65}$ ($a = 0.3846$ nm, $c = 0.4143$ nm, $c/a = 1.07722$ and $V = 0.05307$ nm^3)[27] with expansion of unit cell volume, unit cell in ab-plane and minor compression along c-axis in resulting $Tb_2Ni_{0.90}Si_{2.94}$.

Temperature dependence of dc magnetic susceptibility ($\chi \equiv M/H$) measured in both zero-field-cooled (ZFC) and field-cooled (FC) conditions for 200 Oe applied magnetic field are plotted in Fig. 2(a) with the corresponding temperature derivatives plotted in the right ordinate. The ZFC χ exhibits a broad hump at low temperature region with a maximum at a slightly lower temperature than the spin freezing temperature $T_f = 9.9$ K of the compound, as determined by ac susceptibility measurements, reported earlier[23]. On the other hand, FC χ increases down to the lowest temperature with a saturation tendency in the low-temperature region. The ZFC and FC magnetic susceptibilities diverge from each other below a temperature $T \sim 13$ K, where the FC χ also changes its slope from a diverging PM behaviour towards and saturating tendency. The $d\chi/dT(T)$ curves for both ZFC and FC data exhibits anomaly around 13 K signifying a possible phase transition close to that temperature. Although the zero-field neutron diffraction measurements at $T = 1.7$ K reveal the presence of antiferromagnetic ordering in the system, the overall magnetic susceptibility behaviour of this compound at 200 Oe magnetic field shows typical ferromagnetic-like behaviour and was also observed in many cluster-glass systems[28, 29, 30]. It is quite possible to occur due to the infinitesimally low-field induced metamagnetic transition in this compound. Another possibility is that the ground state of as-cast $Tb_2Ni_{0.90}Si_{2.94}$ is dominated by glassy behaviour. As discussed in ref. [23] on as-cast $Tb_2Ni_{0.90}Si_{2.94}$, the magnetic phase of this compound consists of macroscopically different magnetic phases and AFM spin arrangement is also a part of it with very restricted spatial nature. The magnetization behaviour of FM

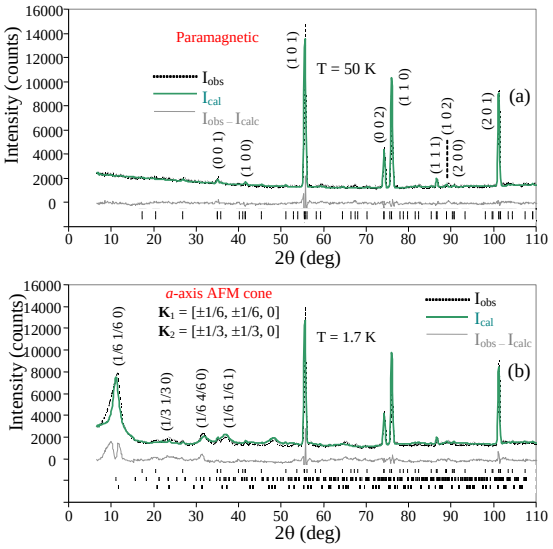

Figure 4: Zero-field neutron diffraction patterns of as-cast $Tb_2Ni_{0.90}Si_{2.94}$ (a) at 50 K (paramagnetic state) and (b) at 1.7 K (in the magnetically ordered state). The first, second, and third rows of ticks refer to the nuclear Bragg peaks and magnetic reflections of k_1, k_2 wave vectors, respectively. The (hkl) of strongest magnetic reflections given in Figure (b)) ($\lambda_1 = 0.24395$ nm, $\lambda_2 = 0.12198$ nm, $I_{\lambda_2}/I_{\lambda_1}$ 0.004).

clusters (those are freezing below 9.9 K) is dominating in the susceptibility behaviour and overwhelms the signal of AFM interactions. Thus, the dominating glassy phase is responsible for the saturation like tendency of M-T behaviour in field-cooled measurement. The estimated effective moment for the compound was 9.7 μ_B/Tb ion with paramagnetic Weiss temperature $\theta_p = 3.9$ K[23]. In case of a pure ferromagnetic system, one would expect Curie temperature $T_C \approx \theta_p$. In the present case, the lower value of θ_p further points toward the presence of antiferromagnetic interaction in the system. The zero-field heat capacity data as shown in Fig. 2(b), also exhibits a broad hump-like features extended over a wide temperature range starting below $\sim$ 20 K. This also signifies that not all the spins in the system are taking part in the antiferromagnetic spin arrangement process simultaneously, implying the magnetic ordering is highly spatially localized in nature, i.e., having very restricted coherence length.

In order to reveal the nature of magnetic ground state spin configuration in as-cast $Tb_2Ni_{0.90}Si_{2.94}$ compound, we have carried out zero-field neutron diffraction measurements at different temperatures as shown in Fig. 3. The feature at the lowest 2θ below 5° in the diffraction patterns are artifacts due to the detector cut-off limit. All the Bragg peaks in the diffraction pattern measured at $T = 50$ K could be well indexed by crystal structure parameters only and thus are of nuclear origin (Fig. 4(a)). Quite a few additional peaks of very weak intensity start to appear in the diffraction pattern for $T \leq 13$ K, which can be expected to be of magnetic origin. The intensity of those additional reflections increase with decrease in temperature. The appearance of the additional Bragg peaks clearly reveal the development of antiferromagnetic spin arrangement in as-cast $Tb_2Ni_{0.90}Si_{2.94}$ compound below $T_N \simeq 13$ K. The AFM interaction is evidenced through neutron diffraction measurements

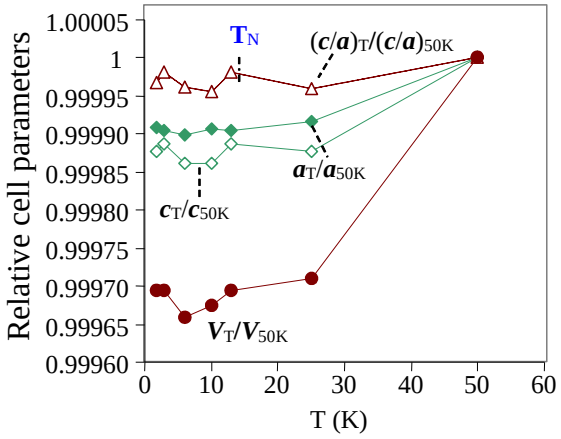

Figure 5: Temperature dependence of the relative cell parameters below 50 K of as-cast $Tb_2Ni_{0.90}Si_{2.94}$. The estimated standard deviation (ESD) of relative cell parameters are smaller than the symbol size.

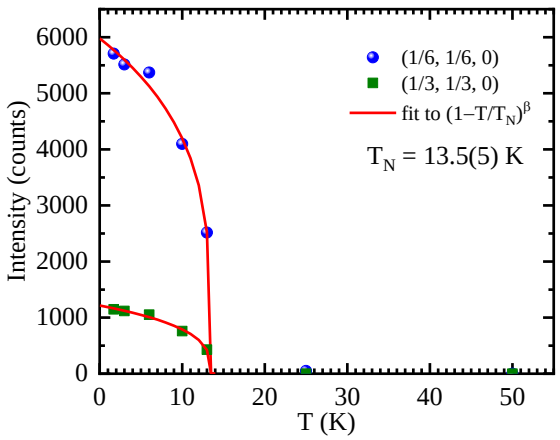

Figure 6: Temperature dependence of the intensity of most intense magnetic Bragg peak of k_1 and k_2 with a power-law fit indicating $T_N = 13.5(5)$ K.

but the very weak intensities of magnetic Bragg peaks and low coherence length suggested by their larger width indicate that those are only limited to a few unit cells of the crystal. The estimated magnetic correlation length from the full width at half maxima(FWHM) of the weak intensity magnetic peaks is found to be only 40 Å at 1.7 K, after correcting the instrument resolution function. The diffraction patterns have further been analyzed with the FULLPROF software package, as shown in Fig. 4(a) and (b) for $T = 50$ K (nuclear) and 1.7 K (nuclear + magnetic), respectively. Although the intensity of the magnetic Bragg peaks are quite weak in nature, those could be indexed with two set of magnetic reflections of $k_1 = [\pm 1/6, \pm 1/6, 0]$ and $k_2 = [\pm 1/3, \pm 1/3, 0]$ wave vectors. Further analysis revealed that from 13 K and down to 1.7 K the magnetic structure of this compound is sum of a-axis sine-modulated component with k_1 wave vector and a-axis flat spiral component with k_2 wave vector. This corresponds to the dominant a-axis antiferromagnetic ordering of Tb sub-

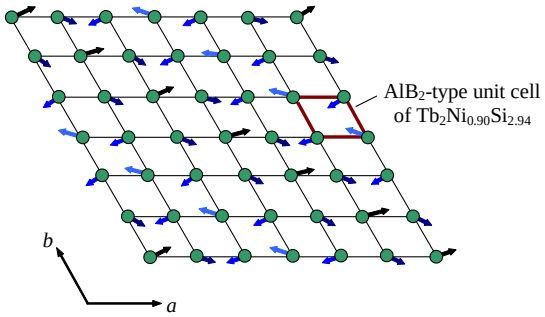

Figure 7: Image of magnetic structure of as-cast $Tb_2Ni_{0.90}Si_{2.94}$ (antiferromagnetic cone with $6a \times 6a \times c$ magnetic unit cell): sum of a-axis sine modulated component with $k_1 = [\pm 1/6, \pm 1/6, 0]$ wave vector and a-axis flat spiral with $k_2 = [\pm 1/3, \pm 1/3, 0]$ wave vector (only Tb sublattice is shown in Figure).

lattice in the $6a \times 6a \times c$ magnetic unit cell. The temperature dependence of the relative cell parameters below 50 K of the compound are plotted in Fig. 5. Fig. 6 depicts the intensity $I(T)$ of most intense magnetic Bragg peaks of k_1 and k_2 as a function of temperature. The experimental data have been fitted with $I(T) \sim (1 - T/T_N)^{\beta}$, that yields $T_N = 13.5(5)$ K and $\beta = 0.36(4)$. The amplitude of terbium magnetic moment with k_1 wave vector M^{k_1} reaches value of $8.9(1)\mu_B$, while flat spiral terbium magnetic moment with k_2 wave vector is $M^{k_2} = 0.68(9)\mu_B$ at 1.7 K, only. The magnetic structure inferred from our zero-field neutron diffraction analysis is shown in Fig. 7.

It is worth mentioning here that the magnetic peaks observed in as-cast $Tb_2Ni_{0.90}Si_{2.94}$ are rather diffusive in nature, similar to that observed in isostructural Er_2NiSi_3 that exhibit reentrant spin glass behaviour below its antiferromagnetic ordering. Such type of diffused magnetic peaks are also earlier observed in many short-range ordered spin-glass compounds[31, 32, 33]. Due to the thermal disruption of magnetic correlation at higher temperature, the diffuse peaks become even broader and weaker as the temperature increases. Our analysis of magnetic structure determination along with this diffuse nature of the magnetic Bragg peaks suggest that the magnetic ground state of the $Tb_2Ni_{0.90}Si_{2.94}$ compound is phase separated in nature and consists of at least three magnetically different macroscopic phases, two antiferromagnetic phases correspond to k_1 and k_2, and another is of glassy in nature existing in a low-dimensional energy scale.

3.1. Summary

Zero-field neutron diffraction measurements have been performed on polycrystalline as-cast $Tb_2Ni_{0.90}Si_{2.94}$ between 1.7 K and 50 K. The system crystallizes in the hexagonal AlB_2-type structure with space group $P6/mmm$. The compound exhibits antiferromagnetic transition below $T_N \sim 13$ K. The magnetic structure of the compound is sum of a-axis sine-modulated component with $k_1 = [\pm 1/6, \pm 1/6, 0]$ wave vector and a-axis flat spiral component with $k_2 = [\pm 1/3, \pm 1/3, 0]$ wave vector. The amplitude of terbium magnetic moment with k_1 wave vector of M^{k_1} reaches value of $8.9(1)\mu_B$, while flat spiral terbium magnetic moment with k_2 wave vector is $M^{k_2} = 0.68(9)\mu_B$ only at 1.7 K. On the basis of magnetization, heat capacity and zero-field neutron diffraction results, we have suggested that the magnetic

ground state of $Tb_2Ni_{0.90}Si_{2.94}$ is magnetically phase separated in nature and comprised of at least two antiferromagnetic phases and one cluster-glass phase of different spatial length scales.

Acknowledgement

This work has been carried out and supported through CMPID-DAE project at SINP. Work at the Ames Laboratory was supported (in part) by the Department of Energy- Basic Energy Sciences, Materials Sciences and Engineering Division: Ames Laboratory, USDOE, under Contract No. DE-AC02-07CH11358. The work carried out by A.V.M. is supported by Russian Fund for Basic Research through the project No. 20-03-00209.

References

[1] Gordon R A, Warren C J, Alexander M G, DiSalvo F J and Pöttgen R 1997 *J. Alloys Comp.* **248** 24
[2] Li D X, Nimori S, Shiokawa Y, Haga Y, Yamamoto E and Onuki Y 2003 *Phys. Rev. B* **68** 012413
[3] Frontzek M, Kreyssig A, Doerr M, Schneidewind A, Hoffmann J-U and Loewenhaupt M 2007 *J. Phys.: Condens. Matter* **19** 145276
[4] Huo D, Sakurai J, Kuwai T, Isikawa Y and Lu Q 2010 *Phys. Rev. B* **64** 224405
[5] Tien C, Luo L and Hwang J S 1997 *Phys. Rev. B* **56** 11710
[6] Majumdar S, Bitterlich H, Behr G, Löser W, Paulose P L and Sampathkumaran E V 2001 *Phys. Rev. B* **64** 012418
[7] Pakhira S, Mazumdar C, Ranganathan R, Giri S and Avdeev M 2016 *Phys. Rev. B* **94** 104414
[8] Pakhira S, Mazumdar C, Ranganathan R and Avdeev M 2017 *Sci. Rep.* **7** 7367
[9] Pakhira S, Kundu A K, Mazumdar C and Ranganathan R 2018 *J. Phys.: Condens. Matter* **30** 215601
[10] Pakhira S, Mazumdar C and Ranganathan R 2017 *J. Phys.: Condens. Matter* **29** 505801
[11] Mo Z J, Shen J, Yan L Q, Gao X Q, Tang C C, Wu J F, Sun J R and Shen B G 2015 *J. Alloys Comp.* **618** 512
[12] Pakhira S, Mazumdar C, Ranganathan R and Giri S 2018 *J. Alloys Comp.* **742** 391
[13] Pakhira S, Mazumdar C and Ranganathan R 2019 *J. Magn. Magn. Mater.* **484** 456
[14] Pakhira S, Mazumdar C and Ranganathan R 2019 *Intermetallics* **111** 106490
[15] Pakhira S, Ranganathan R and Mazumdar C 2020 *J. Magn. Magn. Mater.* **512** 167055
[16] Pakhira S, Kundu M, Mazumdar C and Ranganathan R 2021 *J. Phys.: Condens. Matter* **33** 095804
[17] Kurumaji T, Nakajima T, Hirschberger M, Kikkawa A, Yamasaki Y, Sagayama H, Nakao H, Taguchi Y, Arima Taka-hisa, Tokura Y 2019 *Science* **365** 914
[18] Hirschberger M, Spitz L, Nomoto T, Kurumaji T, Gao S, Masell J, Nakajima T, Kikkawa A, Yamasaki Y, Sagayama H, Nakao H, Taguchi Y, Arita R, Arima T, and Tokura Y 2020 *Phys. Rev. Lett.* **125** 076602
[19] Hirschberger M, Nakajima T, Kriener M, Kurumaji T, Spitz L, Gao S, Kikkawa A, Yamasaki Y, Sagayama H, Nakao H, Ohira-Kawamura S, Taguchi Y, Arima T, and Tokura Y 2020 *Phys. Rev. B* **101** 220401(R)
[20] Pakhira S, Mazumdar C, Ranganathan R and Giri S 2018 *Phys. Chem. Chem. Phys.* **20** 7082
[21] Pakhira S, Mazumdar C, Choudhury D, Ranganathan R and Giri S 2018 *Phys. Chem. Chem. Phys.* **20** 13580
[22] Pakhira S, Mazumdar C, Basu A, Ranganathan R, Bhowmik R N and Satpati B 2018 *Sci. Rep.* **8** 14870
[23] Pakhira S, Mazumdar C, Avdeev M, Bhowmik R N and Ranganathan R 2019 *J. Alloys Comp.* **785** 72
[24] Pakhira S, Bhowmik R N, Avdeev M, Ranganathan R and Mazumdar C 2020 *Intermetallics* **124** 106874

[25] Izumi F 1993 *The Rietveld Method* Edited by R. A. Young (Oxford University Press, Oxford) 13.
[26] Rodríguez-Carvajal J 1993 *Physica B* **192** 55.
[27] Auffret S, Pierre J, Lambert-Andron B, Madar R, Houssay E, Schmitt D, Siaud E, 1991 *Physica B: Condensed Matter* **173** 265.
[28] Li D X, Nimori S, Shiokawa Y, Haga Y, Yamamoto E and Onuki Y 2003 *Phys. Rev. B* **68** 172405
[29] Nam D N H, Jonason K, Nordblad P, Khiem N V, and Phuc N X 1999 *Phys. Rev. B* **59** 4189
[30] Anand V K, Adroja D T, and Hillier A D 2012 *Phys. Rev. B* **85** 014418
[31] Reimers J N 1992 *Phys. Rev. B* **46** 193
[32] Fiorani D, Viticoli S, Dormann J L, Tholence J L, and Murani A P 1984 *Phys. Rev. B* **30** 2776
[33] Tomiyasu K, Fukunaga J, and Suzuki H, 2004 *Phys. Rev. B* **70** 214434